Flash Flood due to Local and Intensive Rainfall in an Alpine Catchment

Shusuke MIYATA,[1,*] Masaharu FUJITA,[1] Takuji TERATANI[2]
and Hirofumi TSUJIMOTO[2]

[1] Disaster Prevention Research Institute, Kyoto University (Ujigawa Open Laboratory, Higashinokuchi, Shimomisu, Yoko-oji, Fushimi, Kyoto 6128235, Japan)

[2] Japan Weather Association (Sunshine 60 Bldg. 55F, 3-1-1Higashi-Ikebukuro, Toshima, Tokyo 1706055, Japan)

*Corresponding author. E-mail: miyata.shusuke.2e@kyoto-u.ac.jp

Rapid increases in stream water level (flash flood) can cause human casualty in mountainous rivers. We attempted to examine effects of spatial distributions of rainfall on occurrences of flash flood in an alpine catchment by combining field observations, application of radar rainfall data, and numerical simulations. Stream water levels at four gauging stations along the main stream and precipitation were observed in the field. Spatial distributions of precipitation were obtained from the C-band radar. Field monitoring results showed quick responses of stream flow even during a prolonged rainfall event. During a short and intensive storm event, stream water level at the outlet of the study site (S1) increased earlier than that that at an upstream gauging station (S2). This earlier response at S1 was associated with the concentration of precipitation in a sub-catchment located between the two gauging stations. Hydrological simulations were conducted for two cases: spatially uniform precipitation (Case 1) and heterogeneous precipitation obtained from the C-band radar (Case 2). Timing and amount of rapid increase in simulated water discharge at S1 under Case 2 corresponded well with observation results. In contrast, increase in stream flow of case 1 was moderate and later than that of observed result. Our simulation results suggest that the rapid increase of stream flow at S1 was contributed not only by the concentrated floods from the sub-catchment due to the localized rainfall but also by water flow from the most upstream of the main channel with thin soil layer.

Key words: radar rain gauge, field observation, numerical simulation, localized intensive rainfall

1. INTRODUCTION

In mountainous areas, human casualty is caused by flash flood, which is defined as rapid increases in stream water level. Although occurrence of flash flood is also known in dry regions with gentle slopes [e.g., *Cohen and Laronne*, 2005; *Borga et al*., 2008], similarity and difference of flash floods in mountain and dry and gentle catchments are still unclear. In Japan, several flash flood disasters have been reported in every year [*Matsuda et al*., 2009; 2010]. Because disasters due to flash flood generally happen in mountainous rivers, it is expected that flash flood phenomenon which do not cause damages and losses frequently takes place [*Kurihara et al*., 2007]. However, there are few observation results of flash flood in the field [e.g., *Kurihara et al*., 2007; *Nagai and Tamura*, 2009].

Previous studies have found several potential factors of flash floods. At Tonami River, Northern Japan, catchment topography with dense stream network enhanced concentration of flood and a flash flood disaster [*Kurihara et al*., 2007]. *Matsuda et al*. [2009] have proposed risk index of flash flood based on the topographic characteristics. Collapse of natural dam sometimes causes flash floods in downstream reaches [*Kurihara et al*., 2007; *Nagai and Tamura*, 2009; *Miyata et al*., 2011]. *Oda et al*. [2009] conducted flume experiments and confirmed that collapse or erosion of small natural dam can cause rapid increases in stream flow. Other potential factor of flash flood is unexpected abundant discharge of groundwater [*Kurihara et al*., 2007].

Despite of potential factors, local and intensive rainstorm can be one of the predominant factors of flash flood [*Matsuda et al*., 2009; 2010]. *Matsuda et al*. [2010] summarized information of flash flood disasters for 10 years and found that all cases of flash flood disasters within river channel were associated with local and/or intensive rainfall.

However, few studies have addressed the relationship between local and intensive rainfall and flash flood based on field monitoring.

It still remains difficulties of predicting potential rivers of flash floods and detail field observations of rainfall and runoff. In mountainous catchments, installation and maintenance of rain-gauge network is very hard and time consuming in mountain catchments. Recently, rainfall data with high spatiotemporal resolutions can be observed using radar technics even in mountain areas. In catchments with high reliefs, field observations for investigating detail hydrological processes are also difficult. We attempted to examine runoff processes within a catchment by applying a numerical simulation. In this study, we examined effects of spatial distributions of rainfall on occurrences of flash flood in an alpine catchment by combining field observations, application of radar rainfall data, and numerical simulations.

2. STUDY SITE AND FIELD OBSERVATION

2.1 Study site

Field observations were conducted in Sugoroku Catchment, which is an incised alpine catchment in central Japan (**Fig. 1**). This catchment was selected because flash flood occurs frequently and sometimes causes human casualties in this catchment. For instance, a climbing and fishing group consisting of three people was washed away and one of the three people dead in 2005. The lower boundary of the catchment was decided to avoid artificial inflow and outflow.

The catchment area is 60.9 km^2 and the elevation ranged from 1207 to 2897 m. Length and average slope of the main stream channel are approximately 14.4 km and 1/10, respectively. The study site with elevations less than 2500 m is covered by forest and dominant tree species is Northern Japanese Hemlock (*Tsuga diversifolia*). In contrast, areas with elevation of greater than 2500 m are covered by bush of Siberian Dwarf Pine (*Pinus pumila*) or grassland of Sasa, or no-vegetation (i.e., bare slope). The study catchment is covered by snow in winter, whereas a part of the catchment is covered by snow even in summer.

2.2 Field observations

Observations of water level and precipitation were conducted in the study catchment (**Fig. 1**). Three rain-gauges, R1-3, were installed close to the catchment boundary and their elevations were about 2560, 2280, 2820 m, respectively. Precipitations

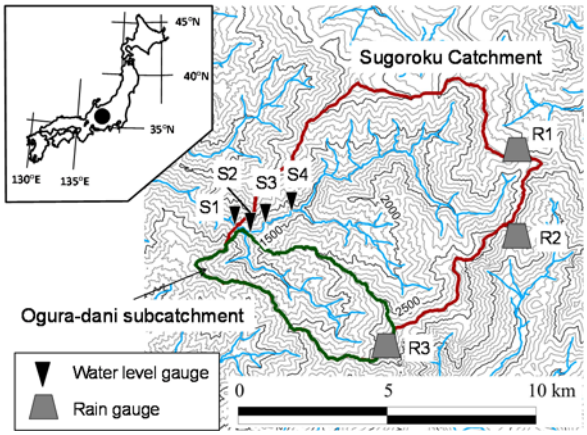

Fig. 1 Location and map of study site

Photo 1 Water level gauge installed at S3 (shown in a white circle)

were observed in the field from August to October in 2011 and 2012. We also used rainfall data observed by a C-band radar rain gauge. Spatial resolution of the radar rainfall data was approximately 1 x 1 km and time resolution was 5 min.

Stream water levels were observed at four gauging stations along the main stream (**Fig. 1**). The most downstream gauging station (S1) corresponds with the outlet of the study catchment. To observe stream water level, pressure sensors were fixed on large cobbles in the stream (**Photo 1**). Water levels were observed every 1-5 minutes and water level observation was conducted from mid-July to early-September in 2012. Stream water levels at S1 and S2 were converted into stream discharges using survey results of stream cross section and the Manning's equation. Manning's coefficient was decided referring previous monitoring results of stream discharge at approximately 100 m downstream of our gauging station S1. The previous monitoring results in 2008 was 1-hr data and used for an investigation of hydrological characteristics of the study catchment.

The gauging stations S1 and S2 were installed to investigate increases in discharge of main channel by stream water from a major sub-catchment, Ogura-dani (shown by green line in **Fig.1**). The

confluence of Ogura-dani and the main channel was located between S1 and S2 (**Fig. 1**).

3. HYDROLOGICAL CHARACTERISTICS AND EFFECTS ON HETEROGENEOUS RAINFALL ON STREAM RUNOFF

3.1 Comparisons of precipitations between rain-gauge and C-band radar

At R1 and R2, hourly precipitations of the C-band radar at meshes in which the rain-gauges were installed generally agreed well with those observed by the rain-gauge on the ground, while precipitation by the C-band radar at R3 was sometimes much greater than that by the rain-gauge (**Fig. 2**). Because the rain-gauges at the high altitudes, especially R3, were exposed by strong wind associated with heavy rainfall, the rain-gauges was possibly not able to capture all of the rainfall. Despite the inconsistency of high precipitation between the C-band radar and the rain-gauges on the ground, the comparisons suggest that the C-band radar is applicable to the study site which has geomorphology of very large relief. Therefore, we use precipitation observed by the C-band radar in the following analyses.

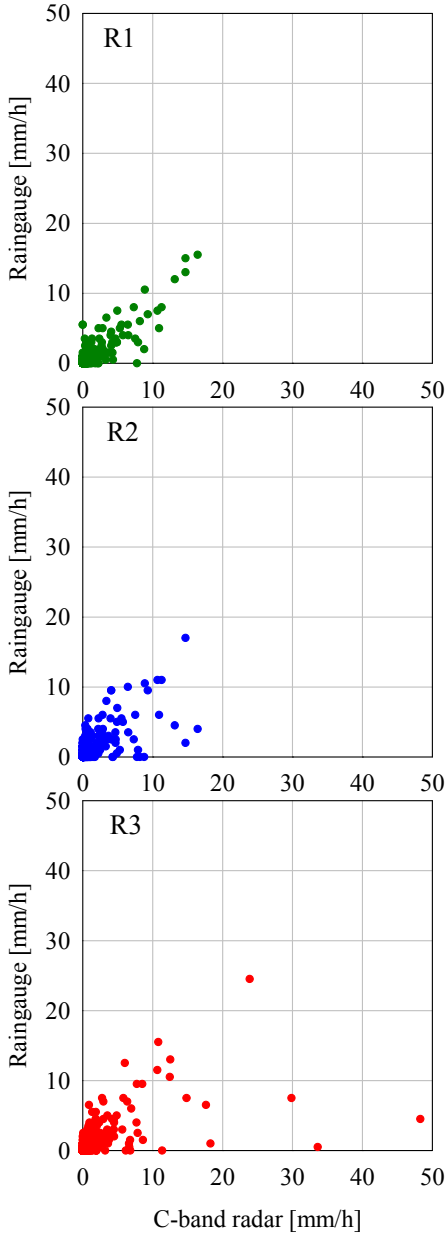

Fig. 2 Comparisons of hourly rainfall between rain-gauge on the ground and C-band radar

3.2 Hydrological characteristics

Runoff coefficient at S1 ranged from 0.016 to 2.0 (**Fig. 3**). A storm event is defined as total rainfall of 20 mm without no-rain period of 12 hours. Total stream discharge in each event was obtained by integrating stream discharge from the start of rainfall to time when stream discharge decreased into the level before the event. In 2008, runoff coefficient tended to be higher in June and then decreased gradually in July (**Fig. 3**). Because snow remained in a part of the catchment with higher elevation in early summer, snow cover may have enhanced low infiltration and high runoff. Snowmelt water also contributed the high runoff coefficient in June.

During a heavy storm in which total rainfall, maximum rainfall intensity and duration were 102.7 mm, 21.7 mm/h and 38.9 hr, respectively, at S1, water levels at the four gauging stations increased and diminished rapidly following changes in rainfall intensity (**Fig. 4**). Water level of S1 started

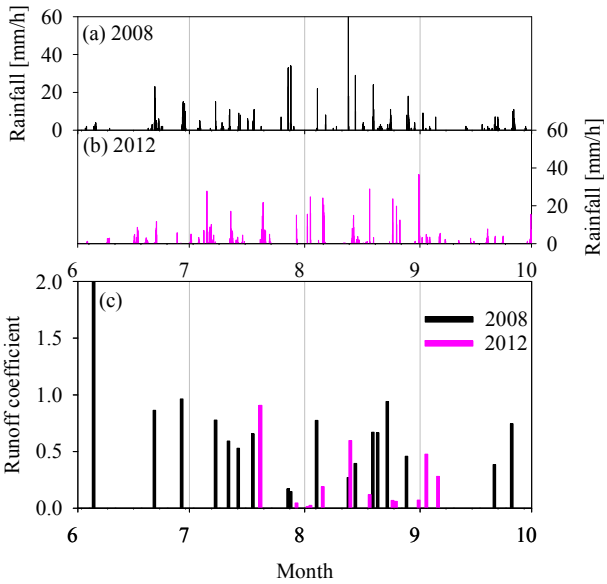

Fig. 3 Temporal changes of rainfall and runoff coefficient in (a) 2008 and (b) 2012

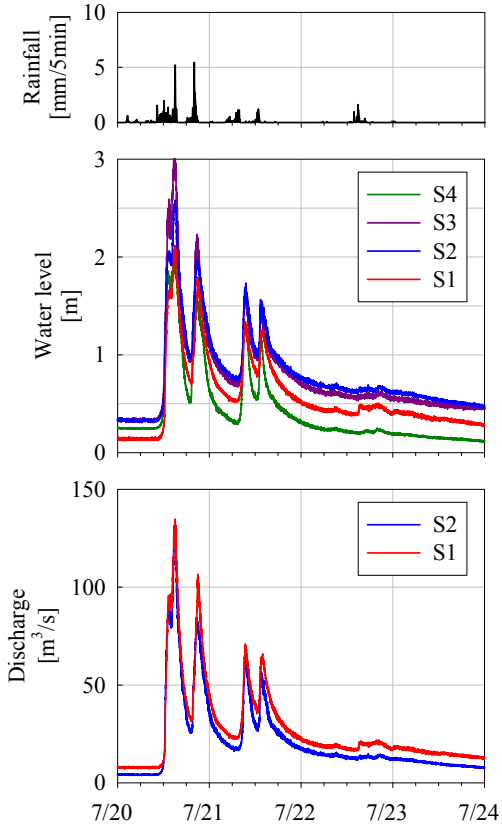

Fig. 4 Temporal changes of rainfall, stream water height and stream discharge at S1 from July 20 to July 23, 2012.

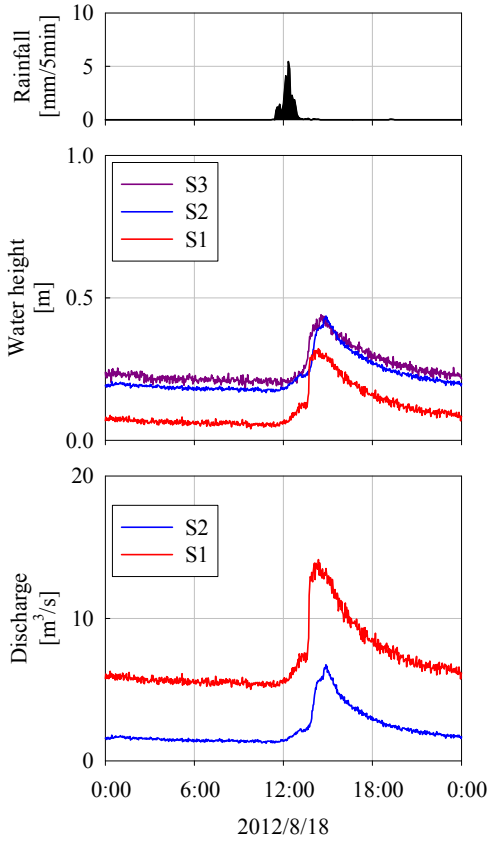

Fig. 5 Temporal changes of rainfall, stream water height and stream discharge at S1 on August 18, 2012.

increasing at 11:00, July 20, 2012 and reached the maximum height of 2.1 m at 15:00, June 20. Then, rapid recession of water level was observed by 19:30, July 20, followed by the second rapid increase of the water level. The maximum stream discharges at S1 was 135 m3/s (= 8.0 mm/h in this catchment). These results suggest the quick runoff responses of the study catchment even during a heavy storm event.

3.3 Rapid increase of stream water associated with local rainfall

Increase in water level at S1was also rapid during a short-duration event (**Fig. 5**). Total precipitation and maximum intensity were 36.7 mm and 28.9 mm/h, respectively, at S1, suggesting that most of the rainfall was applied within 1 hr. Water level of S1 gradually increased from 11:30 and retained from 12:40 to 13:40. The retention of water level was followed by a rapid increase (0.15 m at 13:40 and 0.30 m at 13:54, corresponding to discharges of 6.9 m^3 at 13:40 and 13.2 m^3 at 13:54), despite range of the rising water level was small comparing with the increase of stream water during the July 20 event. Although distance between S1 and S2 was approximately 200 m (**Fig. 1**), increases of water level and discharge at S2 were moderate (2.4 m^3 at 13:40 and 5.5 m^3 at 14:16) comparing with those at S1 (**Fig. 5**).

The differences of runoff response between S1 and S2 resulted in an earlier increase at S1 (i.e., downstream station) comparing with the increase at S2 (i.e., upstream station). Times of peak discharge at S1 and S2 were 14:06 and 14:52, respectively (**Fig. 5**). Therefore, stream water causing the sudden increase at S1 was not delivered via S2 in the main stream channel.

During this short intense event, rainfall was intense especially in the Ogura-dani sub-catchment (**Fig. 6b**). **Figure 6** shows the spatial distributions of maximum 5-min rainfall intensity R_{max} at each mesh of the C-band radar during the prolonged heavy rainfall event on July 20-22 and short intense event on August 18. In the heavy rainfall event on July 20-22, R_{max} ranged from 15.5 to 68.5 mm/h in the study area. In contrast, R_{max} showed wider range of 5.3 - 185 mm/h on August 18. The highest R_{max} was 185 mm/h at two meshes in the Ogura-dani sub-catchment at 12:20, August 18 (**Fig. 6b**). At the two meshed in the Ogura-dani sub-catchment, total precipitations were two times greater than the average of all meshes. Because the outlet of the Ogura-dani sub-catchment was located between S1 and S2 (**Fig. 1**), the locally intense rainfall enhanced

the sudden increase of stream discharge at S1.

4. HYDROLOGICAL MODEL AND SIMULATION CASE

4.1 Model descriptions

To examine rainfall-runoff processes of the study catchment during the short intense storm event, numerical simulations was employed. The simulation model consists of hillslope and stream channel segments (**Fig. 7**). The hillslope segment was divided into 10 x 10 m grids and balances of water in each grid were calculated. In the stream channel simulation, outflows from hillslope grids adjacent to stream channels were used as input.

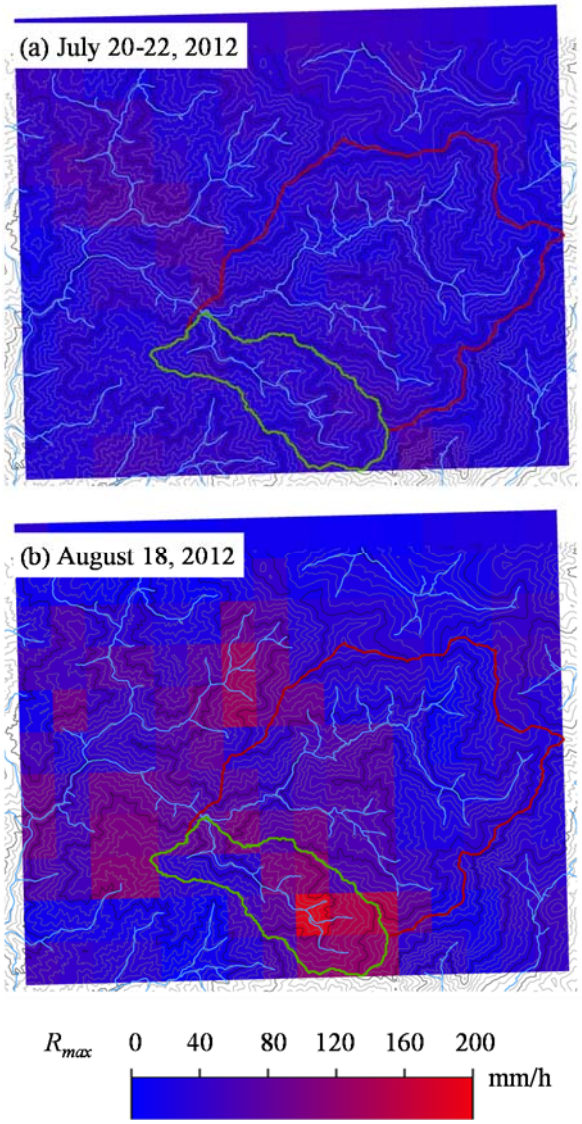

Fig. 6 Spatial distributions of max rainfall intensity during storm events on (a) July 20-23 and (b) August 18, 2012.

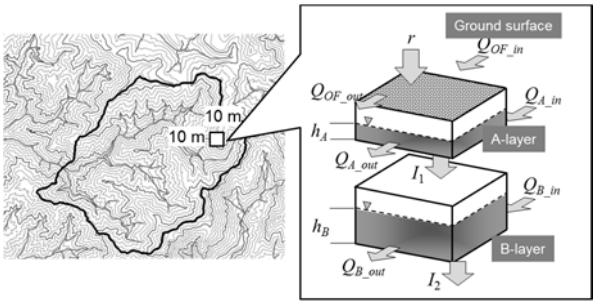

Fig. 7 Schematic illustration of simulation model in hillslope segment.

Based on topography, the Sugoroku catchment was divided into hillslope and stream sections. In the hillslope segment, a grid with the lowest elevation within the neighboring eight grids was defined as flow direction of each 10 x 10 m grid, which consists of A- and B- layers (**Fig. 7**). Rainfall supplied to the surface of each grid infiltrates into A-layer and saturated ground water in the A-layer also infiltrates into the B-layer. Ground water in the B-layer can percolate deeper layer, but the ground water in the deeper layer is assumed not to return to the hillslope nor stream segments.

In this study, we considered overland flow and saturated lateral flows in the two soil layers. Overland flow and saturated lateral flow were calculated using Manning's equation and Darcy's law, respectively. Overland flow at unit width q_{OF} and surface water height h_{OF} were obtained using the following equations.

$$\frac{\partial h_{OF}}{\partial t} + \frac{\partial q_{OF}}{\partial x} = r \tag{1}$$

$$q_{OF} = \frac{\sqrt{i_{OF}}}{n_{sl}} h_{OF}^{5/3} \tag{2}$$

where r is the rainfall intensity, i_{OF} is the hydraulic gradient at the surface, and n_{sl} is the Manning's coefficient (n_{sl}=0.7). Saturated lateral subsurface flow at unit width q_A and ground water height h_A in A-layer were calculated as:

$$\frac{\partial h_A}{\partial t} + \frac{\partial q_A}{\partial x} = q_{in\_A} - q_{in\_B} \tag{3}$$

$$q_A = i_A K_A h_A \tag{4}$$

where q_{in_A} is the infiltration from the surface to A-layer, q_{in_B} is the infiltration from A-layer to B-layer, i_A is the hydraulic gradient in A-layer, and K_A is the saturated hydraulic conductivity of A-layer. Subsurface flow and water height in B-layer were obtained using the same continuum equation and equation of motion.

The one dimensional unsteady flow analysis was applied to simulation of the stream channel segment. Water height h and discharge q in the stream were calculated using the following equations:

$$\frac{\partial h}{\partial t} + \frac{\partial q}{\partial x} = \frac{Q_{in}}{B} \tag{5}$$

$$\frac{\partial q}{\partial t}+\frac{\partial uq}{\partial x}+gh\frac{\partial z}{\partial x}=-gh\frac{\tau}{\rho gR} \quad (6)$$

where B is the channel width, Q_{in} is the inflow from the hillslope segment, u is the average flow velocity, g is the gravity acceleration, z is the water level, τ is the sheer stress at the river bed, ρ is the density of water and the R is the hydraulic radius. Sheer stress is expressed as:

$$\frac{\tau}{\rho}=\frac{gn^2u|u|}{h^{1/3}} \quad (7)$$

These equations were differentiated using the MacCormack method involving the Jameson's artificial viscosity [*Jameson et al*. 1981].

4.2 Simulation case

Hydrological simulations were conducted for the short intense storm event on August 18, 2012. To examine effects of the spatial distribution of rainfall on stream flow, we simulated hydrological processes under two cases of different rainfall data. In Case 1, precipitation at a mesh of downstream area was applied to the entire study catchment for the simulation of hillslope section. That is, spatially uniform rainfall data was used in Case 1. In contrast, radar rainfall data was applied in Case 2, that is, spatial distribution of precipitation was involved. In Case 2, we used precipitation at the closest mesh of the C-band radar as input to a 10 x 10 m mesh in the simulation of the hillslope segment. Simulation period was from August 16 to 18, 2012. Initial conditions of the hillslope and stream flow were given as simulation results of antecedent two weeks.

Based on vegetation covers and their root characteristics, our previous study showed thinner soil depths in areas with elevation greater than 2500 m and approximately 1 m in lower elevation areas [*Miyata et al*., 2012]. In this study, thickness of A-layer was assumed 0 m in areas with elevation greater than 2500 m, whereas that was 0.6 m in the residual areas.

5. SIMULATION RESULTS AND DISCUSSION

In Case 2, the simulation result of discharge at S1 agreed with the observed characteristics (**Fig. 8**), in which retained stream discharge was followed by the sudden increase of discharge (see section 3.3). In both cases, simulated timings at which stream discharges started increasing were agreed with the observation result. In Case 2, the simulated stream flow showed slight changes from 13:25 to 13:45,

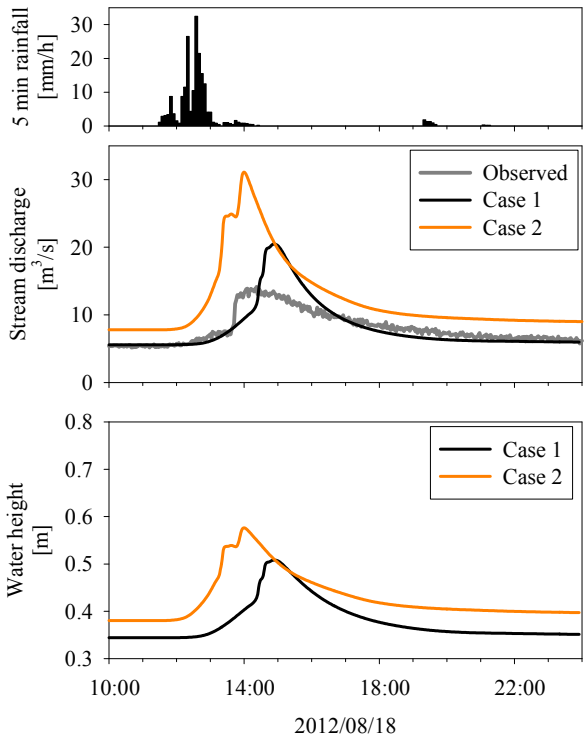

Fig. 8 Simulation results of stream discharge and water height at S1 during August 18event.

followed by the rapid increase of 6.3 m^3/s during 12 min. These timings and range of the rapid increase in discharge in Case 2 were consistent with the observed results.

Simulation results of Case 1 showed moderate rise of stream flow, comparing with that of observed discharge (**Fig. 8**). In Case 1, rising limb of stream flow was longer than the observation result. Thus, simulated time of peak discharge (14:53) was postponed to the observed peak at 14:22.

Longitudinal profiles of stream flow in the main channel and the Ogura-dani show water flows contributing the rapid increases of stream discharge at S1 in Case 2 (shown by arrows in **Fig. 9**). In the Ogura-dani sub-catchment, it was observed the local intensive rainfall (**Fig. 6**), which was converted into substantial increases in stream water from 12:50 and delivered to the main channel between 13:20 and 13:40 (**Fig.9**). However, another rapid increase of stream water delivered from upstream was found in the main channel (shown by black arrows in **Fig. 9**). Absence of A-layer in the upslope area (elevation > 2500 m) probably enhanced concentration of water into upper reach of the main channel, because the upstream end of the main channel had elevation of 2555.5 m. This concentrated stream water reached the downstream end of the main channel at 14:00, which corresponded to timing of the maximum

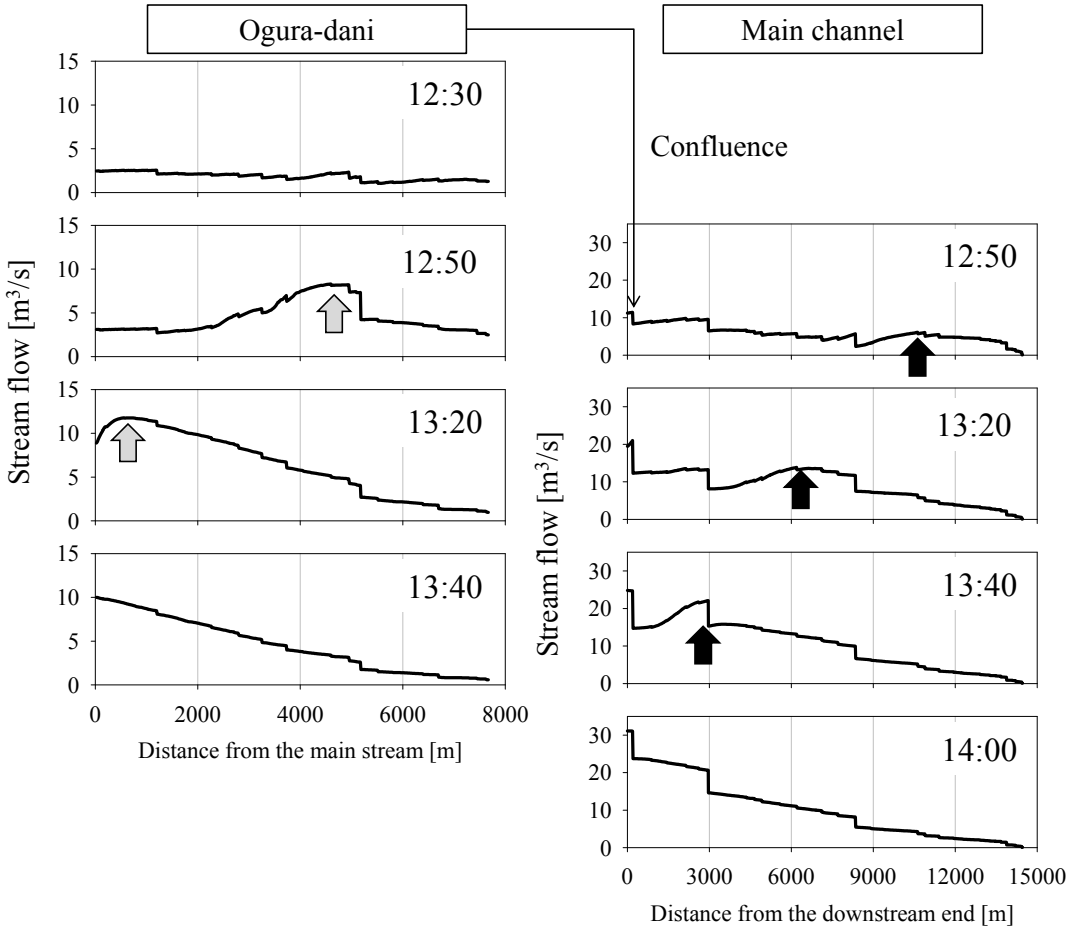

Fig. 9 Longitudinal profiles of stream flow in the Ogura-dani and the main channel during August 18event.

discharge at S1 in Case 2 (**Fig.8**). These simulation results indicate that the rapid increase of stream flow at S1 was associated with the simultaneous arrival of the two concentrated floods from the Ogura-dani and the main channel.

Although our model could simulated the timing of rapid increase of stream discharge with distributed rainfall data (i.e., Case 2), simulated discharge of Case 2 was overestimated (**Fig. 8**). In contrast, simulation result of baseflow in Case 1 was consistent with the observed one. The C-band radar captured rainfall in a part of the study catchment on August 17, while rainfall was 0 mm on August 17 in Case 1. This difference of rainfall data caused higher baseflow in Case 2. The overestimated peak discharge in both cases may be associated with parameters of soil. The parameters were calibrated using discharge data through the observation period. However, snow remains in higher elevation areas generally until early summer, which probably cause high runoff coefficient (**Fig. 3**). Accumulation of observation data without effects of snow over possibly contributes better model validation.

Comparison of the simulated discharge between Cases 1 and 2 also suggest the importance of spatial distribution of rainfall on prediction of flash flood disasters. In our simulation, time when water height at S1 attained to 0.5 m was 79 min earlier in Case 2 (distributed rainfall) than that in Case 1 of uniform rainfall data (**Fig 8**). People within and/or along the river can predict changes in water level based on situation of rainfall where they are. If precipitation is intense only in limited upstream areas as well as the simulated event, people utilizing the river would suddenly face to flash flood before deciding evacuation from the river [*Matsuda et al*., 2010]. Despite the low water height in the simulated event, our simulation approach is applicable to extract rivers which include risk of the flash flood disaster.

6. CONCLUSIONS

To examine effects of spatial distribution of rainfall on flash flood, we conducted field observations of stream water level and rainfall in an incised alpine catchment and applied a distributed hydrological simulation model. The main conclusions are the follows:

1. Water discharges at the four gauging stations increased and diminished rapidly following

changes in rainfall intensity even during a prolonged heavy rainfall event, suggesting inherent characteristics of quick runoff responses of the study catchment.

2. During a short and intensive rainfall event, localized precipitation in a sub-catchment was associated with stream flow response at the outlet of the study site earlier than that at an upstream station.
3. Numerical simulations of runoff processes in the study catchment suggested that the rapid increase of stream flow was contributed not only by the localized rainfall in the sub-catchment but also by runoff from the most upstream of the main channel with thin soil layer.

Our simulation model is expected to apply investigation of flash flood risk of mountainous rivers. Limitations of the model for larger flash floods will be discussed based on observation results.

ACKNOWLEDGMENT: This study was supported by JSPS KAKENHI Grant Number 23780162 to Shusuke Miyata.

REFERENCES

Borga, M., Gaume, E., Creuin, J.D. and Marchi, L. (2008): Surveying flash floods: gauging the ungauged extremes, Hydrological Processes, Vol. 22, pp. 3883-3885.

Cohen, H. and Laronne, J.B (2005): High rates of sediment transport by flashfloods in the Southern Judean Desert, Israel, Hydrological Processes, Vol. 19, pp. 1687-1702.

Jameson, A., Schmidt, W. and Turkel, E. (1981): Numerical solution of the Euler Equations by Finite Volume Methods using Runge-Kutta Time-Stepping Schemes, AIAA 14th Fluid and Plasma Dynamic Conference, pp. 1-19.

Kurihara, J., Takezawa, N., Yamakoshi, T., Tagata, S., Oda, A. and Hasegawa, Y. (2007): Hydrologic characteristics of recent flash floods in mountainous areas in Japan, Journal of Japan Society for Natural Disasters Science, Vol. 26, No. 2, pp. 149-161.

Matsuda, J., Yamakoshi, T. and Tamura, K. (2009): Studies on runoff characteristics of flash flood, Journal of Hydroscience and Hydraulic Engineering, Vol. 53, pp. 487-492.

Matsuda, J., Yamakoshi, T. and Tamura, K. (2010): Studies on alleviation of death accidents by flash floods, Journal of Hydroscience and Hydraulic Engineering, Vol. 53, pp. 487-492.

Miyata, S., Satofuka, Y. and Fujita, M. (2011): Basic investigation of occurrences of flash flood due to collapse of small natural dam, Proceedings of Annual Meeting of Japan Society of Erosion Control Engineering, Vol. 60, pp. 592-593.

Miyata, S., Kobayashi, H., Takebayashi, H., Satofuka, Y., Fujita, M., Tsujimoto, H and Takeshita, W. (2012): Factors affecting runoff characteristics of flash flood in a mountainous stream, Proceedings of Annual Meeting of Japan Society of Erosion Control Engineering, Vol. 61, pp. 148-149.

Nagai, Y. and Tamura, K. (2009): Flash flood triggered by localized intense rainfall – an example observed in Minamiuonuma City, Niigata Japan -, Civil Engineering Journal, Vol. 51, No. 9, pp. 32-37.

Oda, A., Mizuyama, T. and Miyamoto, K. (2009): Experimental study of the shape of small landslide dams during torrents and the discharge hydrograph during an outburst, Journal of Hydroscience and Hydraulic Engineering, Vol. 53, pp. 691-696.